Tip-sample distance control using photothermal actuation of a small cantilever for high-speed atomic force microscopy

Hayato Yamashita,[a] Noriyuki Kodera, and Atsushi Miyagi
Department of Physics, Kanazawa University, Kakuma-machi, Kanazawa 920-1192, Japan

Takayuki Uchihashi, Daisuke Yamamoto, and Toshio Ando
*Department of Physics, Kanazawa University, Kakuma-machi, Kanazawa 920-1192, Japan and CREST, JST,
4-1-8 Honcho Kawaguchi, Saitama 332-0012, Japan*

We have applied photothermal bending of a cantilever induced by an intensity-modulated infrared laser to control the tip-surface distance in atomic force microscopy. The slow response of the photothermal expansion effect is eliminated by inverse transfer function compensation. By regulating the laser power and regulating the cantilever deflection, the tip-sample distance is controlled; this enables much faster imaging than that in the conventional piezoactuator-based z scanners because of the considerably higher resonant frequency of small cantilevers. Using this control together with other devices optimized for high-speed scanning, video-rate imaging of protein molecules in liquids is achieved. © *2007 American Institute of Physics.* [DOI: 10.1063/1.2766825]

I. INTRODUCTION

Atomic force microscopy (AFM) has the unique capability to image biomolecules under physiological conditions at a high spatial resolution.[1,2] If the imaging rate of the AFM is enhanced significantly, this unique capability will become more useful in biological sciences because it enables us to practically observe the dynamic behavior of biological macromolecules. Therefore, various efforts have been made to increase the scan speed.[3–11] In addition, some efforts have been made to reduce the tip-sample interaction force without reducing the scan speed in the tapping mode.[10] Owing to these efforts, the feedback bandwidth has increased to approximately 70 kHz, thereby enabling the capture of moving protein molecules on video at ~48 ms/frame for a scan range of ~240 nm without damaging them.[8,10]

To widen the scope of biological systems whose dynamic behaviors can be studied by high-speed AFM, efforts toward further enhancement of the imaging rate are required. Among the various modes, tapping mode operates most gently on biological samples. This is because, in this mode, the oscillating tip exerts very small lateral forces onto the sample as long as the feedback bandwidth is sufficiently high to facilitate the tip to accurately trace the sample topography.[12] However, the feedback bandwidth is limited by various factors. The slowest device in the feedback loop is the z scanner because the capacity of the available piezoactuators is limited. The response speed of the z scanner is approximately expressed by $\pi f_s / Q_s$, where Q_s and f_s are the quality factor and resonant frequency of the z scanner, respectively. Although Q_s can be reduced to 0.5 by an active damping technique,[8] f_s is almost determined by the required maximum displacement and hardly exceeds ~200 kHz in practice.

In order to overcome this problem, instead of a conventional piezoactuator-based z scanner, a cantilever deflection can be used to control the tip-sample distance because it is easier to increase the resonant frequency of the cantilever than that of the piezoelectric actuator. One possible technique is the magnetic actuation of a cantilever.[13] However, when the cantilever is coated with a magnetic material, its resonant frequency reduces and it also becomes stiff, which is inappropriate for high-speed imaging on biological samples. Another possible technique is to actuate the cantilever by laser illumination onto the cantilever. There are several reports in which an intensity-modulated laser beam is irradiated onto a cantilever for actuation.[14–17] This actuation is based either on the irradiation pressure or on the photothermal expansion with gold-coated cantilevers.[15] In liquids, the latter effect is dominant because of the low quality factor of cantilevers. Although some studies have employed the photothermal effect for exciting resonant vibrations in cantilevers, this effect has never been used in controlling the tip-sample distance. This is because of the slow response of the photothermal bending of cantilevers due to the slow heat transmission.[16] In this study, we have solved this problem by using an inverse transfer function compensation.

II. EXPERIMENTS

A. Apparatus

The in-house developed high-speed AFM apparatus used in this study is basically the same as that reported previously.[4] The optical beam deflection method optimized for small cantilevers was used. In order to detect the cantilever deflection and drive the cantilever simultaneously, we implemented a 980 nm IR laser as well as a 675 nm red laser, as shown in Fig. 1. Beams from the red and IR lasers were introduced into a ×20 objective lens and focused onto a small cantilever with a length of 6–7 μm, width of 2 μm,
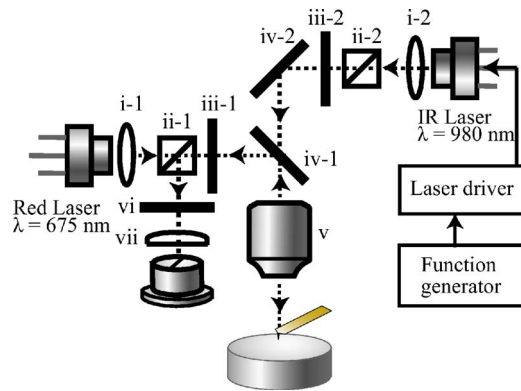
[a]Electronic mail: yhayato@stu.kanazawa-u.ac.jp

FIG. 1. (Color online) AFM with two laser beams of different wavelengths. Schematic diagram for the optical system of the AFM. The linearly polarized beams from a red laser diode (675 nm) or an IR laser diode (980 nm) are collimated by the respective collimation lenses (i-1, i-2), passed through the respective polarization splitters (ii-1, ii-2), and circularly polarized by the respective $\lambda/4$ wave plates (iii-1, iii-2); then, they enter an objective lens (v) after being reflected by or transmitted through a dichroic mirror (iv-1, iv-2). The beams reflected back by a small cantilever are separated by the same dichroic mirror (iv-1). The reflected red laser beam is guided into a split photodiode through the polarization splitter (ii-1), a band-pass filter (vi), and a spherical planoconvex lens (vii).

FIG. 2. DC displacement of the cantilever as a function of the IR laser power.

and thickness of 90 nm (resonant frequency: ~1.2 MHz in water; spring constant: ~0.2 N/m). The backside of the cantilever is coated with gold of thickness less than 20 nm. The irradiation position of the IR laser onto the cantilever was adjusted so that maximum cantilever deflection was attained. An optical band-pass filter with 97% transmission at 675 nm and $3 \times 10^{-4}\%$ transmission at 980 nm was positioned in front of the deflection sensor to prevent the interference of the IR laser with the deflection sensing of the red laser. The power of the IR laser was modulated using a laser driver (ALP-6133LA, Asahi data systems, Kanagawa, Japan) that is capable of modulating the laser power up to 200 mW with a frequency in the range of 0–10 MHz. However, the maximum laser power illuminated was reduced down to approximately 100 mW after the IR laser beam passed through the objective lens because the IR laser beam was partly eclipsed at the objective lens inlet. When the gold-coated surface of the cantilever is illuminated, the light absorption induces a bimetal action due to heating; this in turn causes the cantilever to bend away from the light source because gold has a greater heat-expansion coefficient than silicon nitride. Figure 2 shows the cantilever displacement as a function of the laser power. The cantilever bends in proportion to the dc power change to approximately 60 nm. The laser power indicated in Fig. 2 is not the one actually absorbed by the cantilever but that measured at the exit of the objective lens. The light absorption by gold at 980 nm is very small and the spot size of the IR laser focused onto the cantilever is about two times greater than the cantilever width. Therefore, the absorbed power should be much smaller than that indicated in Fig. 2. The effective displacement efficiency was 1.1 nm/mW.

B. Inverse transfer function compensation

Figure 3(a) shows the frequency spectra of the cantilever oscillation induced by the photothermal actuation in water. It should be noted that the decrease in both the measured gain
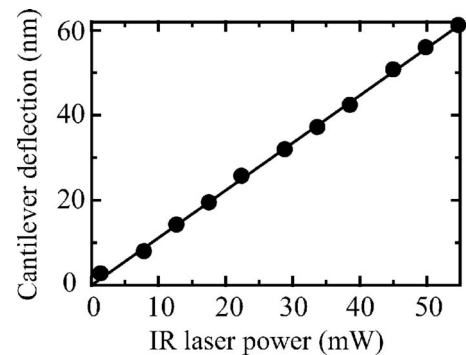
and phase responses (solid lines) is already significant around 10 kHz, which is not consistent with the theoretical curves (dotted lines) for the harmonic oscillator. This is because the temperature variation at the illuminated position and the thermal diffusion length decrease as the modulation frequency increases.[16] In order to utilize the optically driven bending of the cantilever for a faster control of the tip-sample distance, it is essential to eliminate the response delay in the photothermal effect. This can be accomplished by inverse transfer function compensation.[18] The time-domain response of the cantilever to the laser power modulation with a rectangular wave is shown in Fig. 3(b). The cantilever response can be well fitted by a double-exponential function using time constants of 8.4 and 123 μs as drawn by a solid line in Fig. 3(b). Therefore, the transfer function $G(s)$ of the photothermal response of the cantilever is approximately expressed as $G(s) = A/(1+s/\omega_1) + B/(1+s/\omega_2)$ $(A+B=1)$. The equivalent circuit with the transfer function $G(s)$ is the parallel connection of two low-pass filters with time constants of $1/\omega_1$ and $1/\omega_2$. We created the inverse transfer function $1/G(s)$ by using the circuit shown in Fig. 4.[18] In Fig. 4(a), $G(s)$ represents the equivalent circuit for the photothermal response of the cantilever. The transfer function $M(s)$ of this circuit is expressed by $M(s) = 1/[1 + g(G(s) - 1)]$. In the case of $g=1$, a complete inverse transfer function [i.e., $M(s) = 1/G(s)$] can be realized. However, in practice there are some delays in the electronic components such as operational amplifiers. Therefore, the gain factor g should be less than 1, and as a result, the complete inverse transfer function cannot be realized. In order to improve the incomplete inverse transfer function, we used a double loop circuit, as shown in Fig. 4(b). Figure 5 shows the frequency spectra of the cantilever optically actuated under the inverse transfer function compensation. The gain response is consistent with the theoretical curve even at the resonant frequency. The phase signal is delayed at frequencies higher than 400 kHz because of incomplete compensation. However, the frequency that yields a 45° phase delay is about 700 kHz, which is approximately five times higher than that of our piezoactuator-based z scanner.[8]

C. Feedback bandwidth

The feedback performance of our tapping-mode AFM with a photothermally driven cantilever was evaluated.
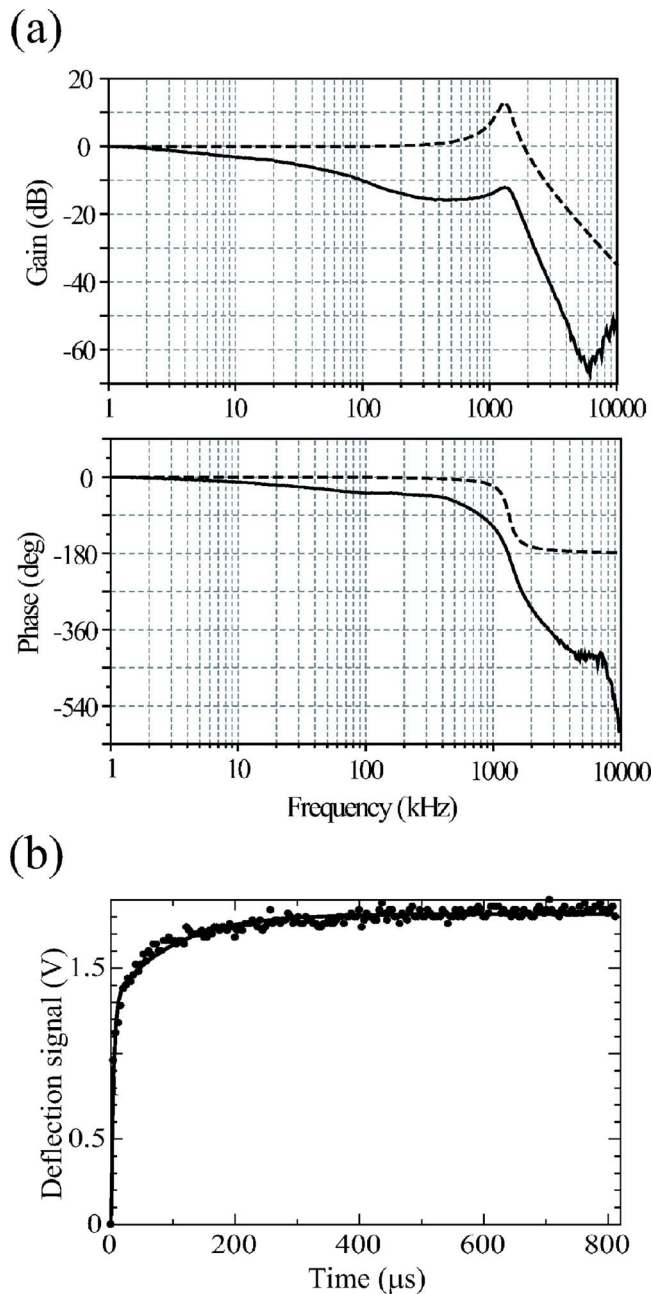
(a)

(b)

FIG. 3. (Color online) (a) Frequency spectra of the gain (upper) and phase (lower) for a small cantilever excited by the intensity-modulated IR laser (solid lines) and theoretical frequency spectra for harmonic oscillation (dotted lines). The cantilever amplitude was $10 \mathrm{nm}_{\mathrm{p-p}}$. (b) The time-domain response of the cantilever displacement driven by the laser modulated with a rectangular wave. The response shown with dots is fitted by a double-exponential-function curve (solid line), $\alpha[1-\exp(-t/\tau_1)] + \beta[1-\exp(-t/\tau_2)]$ with time constants of $\tau_1 \sim 8.4 \ \mu s$ and $\tau_2 \sim 123 \ \mu s$.

Herein, a small cantilever was oscillated using a piezoactuator at its resonant frequency of 1.2 MHz in water ($Q=3$), with a free oscillation amplitude of 5 nm. The tip was intermittently contacted with a mica surface in water, with an average amplitude of 3 nm. The cantilever deflection was modulated by sinusoidal signals, and the output signals from the proportional-integral-differential (PID) circuit were monitored for the closed loop. Here, the modulation frequencies are much lower than the cantilever resonant frequency. The parameters of the PID controller were adjusted to
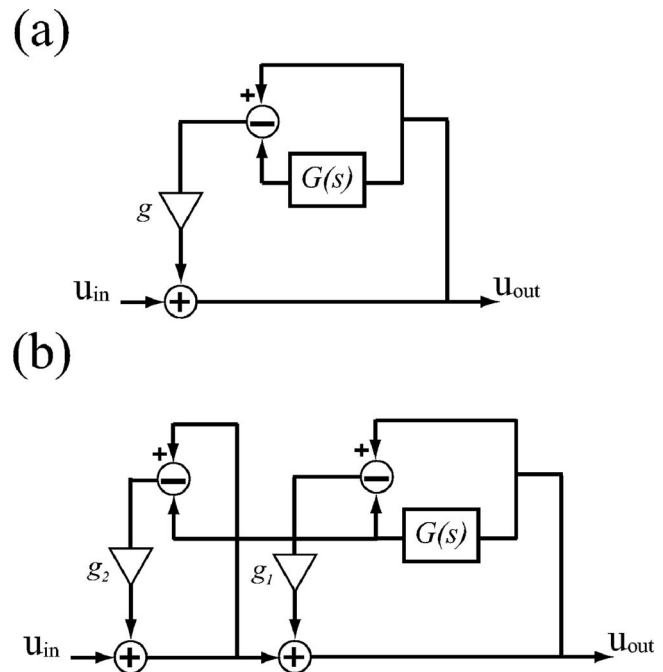
(a)

(b)

FIG. 4. Block diagrams of delay compensation circuits with a single loop (a) and a double loop (b).

achieve the best feedback condition. Figure 6 shows a closed-loop transfer function with the cantilever actuation. The feedback bandwidth, which is defined as the frequency that yields 45° phase delay, was approximately 100 kHz as indicated in Fig. 6 (dotted line). This value is higher by a factor of 1.4 in comparison to the tip-sample distance control by our piezoactuator-based z scanner.[8] Here, although the gain response shows peaks around 100 and 500 kHz, the gain values at the peaks are less than 3 dB, which is the
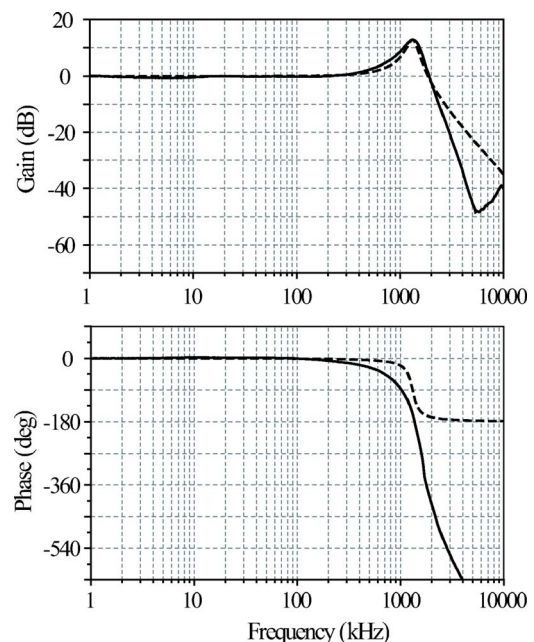

FIG. 5. (Color online) Frequency spectra of the gain (upper) and phase (lower) for a small cantilever excited by the intensity-modulated IR laser with delay compensation and theoretical frequency spectra for harmonic oscillation (dotted lines).
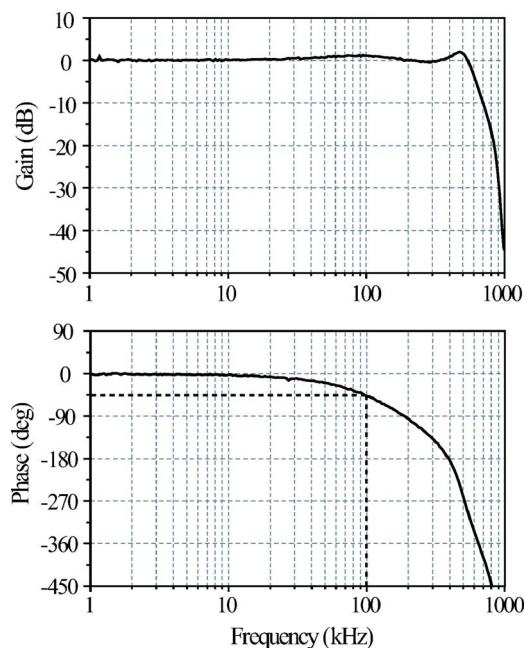
FIG. 6. (Color online) Frequency spectra of the closed-loop transfer function for the cantilever actuation. While the tip was intermittently contacted the surface and then the cantilever deflection was modulated by sinusoidal signals, the output signals from the PID circuit were monitored for the closed loop. The feedback bandwidth was defined at the frequency with the 45° phase delay.

tolerance for the AFM feedback condition.[8] The feedback bandwidth of 100 kHz is expected to achieve a video-rate (33 ms/frame) imaging because an imaging rate of 48 ms/frame was previously achieved with a feedback bandwidth of 70 kHz.[8,10]

III. IMAGING OF BIOLOGICAL MOLECULES

The increase in temperature of the cantilever and the irradiation of the intense laser light onto the biological samples may damage the proteins. In fact, we had previously observed that a violet laser (405 nm) irradiation denatured proteins such as myosin V and actin filaments. On the other hand, the IR laser is widely used for optical trapping technique to manipulate biological molecules.[19] In the optical trapping system, the IR laser with power higher than 100 mW is usually used and still biological molecules are not significantly denatured.[20] Liu *et al.* have reported that the temperature rise of a lipid directly irradiated by the IR laser with 100 mW and a focused spot size of 0.8 μm in water is about 1.5 °C.[21] In our system, the spot size is larger (>1 μm) for 100 mW and most of the laser illuminates the cantilever, which is separated from the surface about 1 μm. Therefore it is expected that the IR laser does not rise sample temperature so much. In fact, obvious structural alterations of proteins were not observed when an IR laser was used. Fig. 7 shows the gliding movement of actin filaments over a myosin V-coated surface[22] in the presence of adenosine triphosphate (ATP). The focused IR laser with a power of 100 mW was irradiated onto the small cantilever while imaging. Figs. 7(a)–7(c) are shown every five frames for the images obtained at 970 ms/frame. One can see actin filaments gliding on the substrate; the ends of the actin fila-
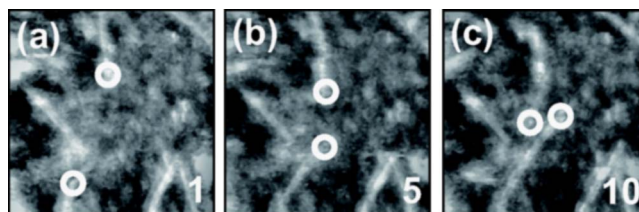

FIG. 7. (Color online) AFM images of actin filaments gliding on myosin V under the laser excitation. The images were acquired at 970 ms/frame but showed every five frames (as shown by lower number). The scan area and pixel size are 800 × 800 nm^2 and 200 pixel^2, respectively. The ends of the actin filament gliding are indicated by open circles.

gliding are highlighted by open circles. Also, apparent structural damage of myosin V under the IR laser irradiation was not seen as described later. From this result, we can conclude that the IR laser beam does not significantly damage the activities of the proteins under the optical configuration used in the AFM observation.

Figure 8 compares the imaging performance by the photothermal control of the tip-sample distance with that in our piezoactuator-based z scanner[8] by using a soft sample (myosin V molecules). The scan speed was set to attain 31 ms/frame for a 240 nm scan range and 100 scan lines. The sample was prepared in the same manner as described before.[23] Figures 8(a) and 8(b) show the AFM images obtained using the photothermally driven cantilever. In these images, a typical myosin V structure having two heads followed first by long neck regions and then by a coiled-coil tail is evident. Even after approximately 7 s (i.e., after imaging 233 times), no significant structural damages are visible, as shown in Fig. 8(b). On the other hand, by using the piezoactuator-based z scanner to control the tip-sample distance, the spatial resolution of the image is obviously deteriorated. Moreover, the myosin V molecules are disrupted due to the very strong tip force caused by the insufficient
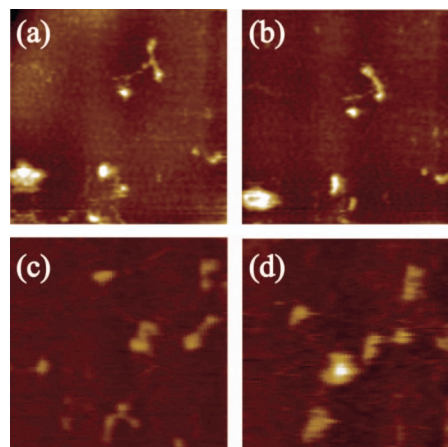

FIG. 8. (Color) AFM images of myosin V on mica in a buffer solution obtained by photothermally driving the cantilever [(a) and (b)] or by using a piezoactuator-based z scanner [(c) and (d)]. The scan area is 240 × 240 nm^2. The frame rate was 31 ms/frame for all the images. Images (a) and (c) are taken at the beginning of imaging and images (b) and (d) are taken at around 7 and 3 s, respectively.

feedback bandwidth, as shown in Fig. 8(c). Furthermore, after a few seconds, the myosin V molecules are aggregated, as shown in Fig. 8(d).

IV. DISCUSSION

We have presented a novel technique to control the tip-sample distance by utilizing the photothermal bending of the cantilever. By characterizing the transfer function of the photothermal response of the cantilever and composing a circuit with the inverse transfer function of the delay of the photothermal bending, we eliminated the slow photothermal response of the cantilever motion. By using this technique, we succeeded in the video-rate imaging of myosin V molecules without damaging them. This technique can easily increase the feedback bandwidth in AFM without modifying the cantilever and piezoelectric actuator. At the moment such high feedback bandwidth cannot be achieved by using a piezoelectric actuator although the fast feedback control is essential in tracing precise surface topography and realizing noninvasive imaging on biological samples. A drawback of this method may be the limitation of the maximum deflection of the cantilever ($\sim$100 nm) due to the small deflection efficiency (1.1 nm/mW) for the low frequency ($<$1 kHz) power change and the maximum power (100 mW) of the IR laser used. At the moment, the maximum actuation range is about 34 nm for the sample with the spatial frequency less than 100 kHz, which is the limited feedback bandwidth, because one needs about three times power to compensate the gain reduction of 10 dB at the frequency of 100 kHz from Fig. 3(a). This can be improved by combining a piezoelectric actuator that operates only for a low-frequency topography or by using an IR laser with a higher power. Although the bandwidth for the open loop transfer function is five times higher than that for our piezoactuator-based z scanner,[8] the feedback bandwidth did not improve as much as expected from the bandwidth of the "cantilever scanner". This is because the quality factor of the cantilever is approximately 3 in water, while the quality factor of the piezoelectric actuator is reduced to approximately 0.5 when the active damping technique is used.[8] By reducing the quality factor of the cantilever with an active Q-control method, faster imaging beyond the video rate could be achieved in the near future.

[1] M. Radmacher, M. Fritz, H. G. Hansma, and P. K. Hansma, Science **265**, 1577 (1994).
[2] D. J. Müller, H. Janovjak, T. Lehto, L. Kuershner, and K. Anderson, Prog. Biophys. Mol. Biol. **79**, 1 (2002).
[3] T. Sulchek, R. Hsieh, J. D. Adams, S. C. Minne, C. F. Quate, and D. M. Adderton, Rev. Sci. Instrum. **71**, 2097 (2000).
[4] T. Ando, N. Kodera, E. Takai, D. Maruyama, K. Saito, and A. Toda, Proc. Natl. Acad. Sci. U.S.A. **98**, 12468 (2001).
[5] T. Ando, N. Kodera, D. Maruyama, E. Takai, K. Saito, and T. Ando, Jpn. J. Appl. Phys., Part 1 **41**, 4851 (2002).
[6] A. D. L. Humphris, M. J. Miles, and J. K. Hobbs, Appl. Phys. Lett. **86**, 1 (2005).
[7] T. Ando, N. Kodera, T. Uchihashi, A. Miyagi, R. Nakakita, H. Yamashita, and K. Matada, e-J. Surf. Sci. Nanotechnol. **3**, 384 (2005).
[8] N. Kodera, H. Yamashita, and T. Ando, Rev. Sci. Instrum. **76**, 053708 (2005).
[9] G. E. Fantner *et al.*, Ultramicroscopy **106**, 881 (2006).
[10] N. Kodera, M. Sakashita, and T. Ando, Rev. Sci. Instrum. **77**, 083704 (2006).
[11] P. K. Hansma, G. Schitter, G. E. Fantner, and C. Prater, Science **314**, 601 (2006).
[12] P. K. Hansma *et al.*, Appl. Phys. Lett. **64**, 1738 (1994).
[13] G. R. Jayanth, Y. Jeong, and C.-H. Menq, Rev. Sci. Instrum. **77**, 053704 (2006).
[14] N. Umeda, S. Ishizaki, and H. Uwai, J. Vac. Sci. Technol. B **9**, 1318 (1991).
[15] O. Marti, A. Ruf, M. Hipp, H. Bielefeldt, J. Colchero, and J. Mlynek, Ultramicroscopy **42–44**, 345 (1992).
[16] D. Ramos, J. Tamayo, J. Mertens, and M. Calleja, J. Appl. Phys. **99**, 124904 (2006).
[17] S. S. Verbridge, L. M. Bellan, J. M. Parpia, and H. G. Craighead, Nano Lett. **6**, 2109 (2006).
[18] G. F. Franklin, J. D. Powell, and A. Emami-Naeini, *Feedback Control of Dynamic Systems*, 5th ed. (Prentice Hall, New Jersey, 2005).
[19] A. Ashkin and J. M. Dziedzic, Science **235**, 1517 (1987).
[20] S. Uemura, H. Higuchi, A. O. Olivares, E. M. De La Cruz, and S. Ishiwata, Nat. Struct. Mol. Biol. **11**, 877 (2004).
[21] Y. Liu, D. K. Cheng, G. J. Sonek, M. W. Berns, C. F. Chapman, and B. J. Tromberg, Biophys. J. **68**, 2137 (1995).
[22] T. Ando, T. Uchihashi, N. Kodera, A. Miyagi, R. Nakakita, H. Yamashita, and M. Sakashita, Jpn. J. Appl. Phys., Part 1 **45**, 1897 (2006).
[23] H. Koide, T. Kinoshita, Y. Tanaka, S. Tanaka, N. Nagura, G. Meyer zu Hörste, A. Miyagi, and T. Ando, Biochemistry **45**, 11598 (2006).